HHS Public Access

Author manuscript

*Cancer Res*. Author manuscript; available in PMC 2017 March 15.

Published in final edited form as:

*Cancer Res*. 2016 March 15; 76(6): 1348–1353. doi:10.1158/0008-5472.CAN-15-1150.

# Dynamic patterns of clonal evolution in tumor vasculature underlie alterations in lymphocyte-endothelial recognition to foster tumor immune escape

**Daniel M. Corey**[1,2,*], **Yuval Rinkevich**[2], and **Irving L. Weissman**[2,3,*]

[1]Department of Hematology, Stanford University School of Medicine, Stanford, Ca 94305, USA

[2]Stanford Ludwig Center for Cancer Stem Cell Research and Medicine, Stanford University School of Medicine, Stanford, Ca 94305, USA

[3]Departments of Pathology and Developmental Biology, Stanford University School of Medicine, Stanford, Ca 94305, USA

## Abstract

While tumor blood vessels have been a major therapeutic target for cancer chemotherapy, little is known regarding the stepwise development of the tumor microenvironment. Here, we use a multicolor Cre-dependent marker system to trace clonality within the tumor microenvironment to show that tumor blood vessels follow a pattern of dynamic clonal evolution. In an advanced melanoma tumor microenvironment, the vast majority of tumor vasculature clones are derived from a common precursor. Quantitative lineage analysis reveals founder clones diminish in frequency and are replaced by sub-clones as tumors evolve. These tumor specific blood vessels are characterized by a developmental switch to a more invasive and immunologically silent phenotype. Gene expression profiling and pathway analysis reveals selection for traits promoting upregulation of alternative angiogenic programs such as unregulated HGF- MET signaling, and enhanced autocrine signaling through VEGF and PDGF. Furthermore, we show a developmental switch in the expression of functionally significant primary lymphocyte adhesion molecules on tumor endothelium, such as the loss in expression of the mucosal addressin MAdCAM-1—whose counter receptor a4β7 on lymphocytes controls lymphocyte homing. Changes in adhesive properties on tumor endothelial subclones are accompanied by decreases in expression of lymphocyte chemokines CXCL16, CXCL13, CXCL12, CXCL9, CXCL10, and CCL19. These evolutionary patterns in the expressed genetic program within tumor endothelium will have both a quantitative and functional impact on lymphocyte distribution that may well influence tumor immune function and underlie escape mechanisms from current anti-angiogenic pharmacotherapies.

[*]Corresponding authors: Daniel Corey, AACR Membership #: 334668, Lokey Stem Cell Research Building, 265 Campus Drive #G3165, Stanford, CA 94305, Tel: 650-723-6520 Fax: 650-723-4034, dcorey@stanford.edu Irv Weissman, Lokey Stem Cell Research Building, 265 Campus Drive #G3165, Stanford, CA 94305, Tel: 650-723-6520 Fax: 650-723-4034, irv@stanford.edu.

We have read and understood CancerResearch policy on declaration of interests and declare that we have no competing interests.

## Introduction

Clonal selection of somatic and germ line stem cells, through competitive interactions, is a common feature of tissue development [1–6]. While genomic analysis of the clonal origins of tumor cells have begun to map the evolutionary relationships responsible for cancer clone maintenance and propagation, little is known regarding the stepwise progression of the tumor microenvironment. Recent evidence suggests the tumor microenvironment, in particular the vascular compartment, promotes tumor maintenance, and may have a role in promoting therapeutic resistance. In a variety of tumors, subsets of highly tumorigenic cells have been found to exist in close proximity to tumor endothelium [7, 8]. This interaction has been shown to be reciprocal; tumors can remodel tissue microenvironments and specialized niches to their competitive advantages. Here we investigate the stepwise development of the tumor microenvironment via genetic fate mapping, lineage tracing, and gene expression profiling. We demonstrate that the clonal architecture within developing tumor microenvironments undergoes dynamic changes, with a bias toward mono- to oligoclonality as tumors progress. Indeed, the loss of founder clones associated with tumor disease progression, is followed by the acquisition of genetic traits in surviving sub-clones characterized by a loss in expression of functionally significant primary lymphocyte adhesion and chemokine molecules, and upregulation of cell-autonomous growth signaling and alternative angiogenic programs. These findings are in contrast to the clonal architecture and gene expression programs of homeostatic endothelium, which exists in a quiescent, polyclonal state. We therefore describe a developmental switch in the stepwise progression of tumor vasculature from a restricted set of progenitors to clonally selected subclones. The consequence of these endothelial changes we propose will have both a quantitative and functional impact on lymphocyte distribution that may well influence tumor immune function and underlies pharmacologic escape mechanisms from current anti-angiogenic therapies.

## Material and Methods

### Mice

Mice were bred and maintained at Stanford University Research Animal Facility in accordance with Stanford University guidelines. Rosa-26 rainbow mice were generated as previously described [2]. ActinCreERT2 transgenic and VE-cadherin-CreERT2 were obtained from the Jackson Laboratory and crossed to homozygous Rosa-26 Rainbow. Briefly, for Cre induction, 10 week-old mice were injected intraperitoneally with a total of 4–6 mg of tamoxifen i.p. every other day for five days (three injections).

### Induction of Angiogenesis in Mice by Syngeneic B16 Melanoma Tumors

The B16-F1 melanoma cell line was obtained from ATCC in July 2012 and maintained in DMEM supplemented with 2 mM L-glutamine, 100 units/ml penicillin, 100 μg/ml streptomycin, and 10% fetal bovine serum (PromoCell). To induce tumor angiogenesis, the mice were injected subcutaneously with B16 cells ($5 \times 10^4$ cells in 20 μl), five days following Tamoxifen administration, and tumors were allowed to grow for 7–40 days.

### Tumor Tissue and Blood Vessel Dissociation

Tumor tissues were mechanically dissociated in Medium 199 containing Liberase TM and TH enzymes (Roche), DNase (Worthington) and Pluronic-F68 (Sigma) at 37°C until single-cell suspension was achieved (2–6 h). Cells were then washed twice with phosphate-buffered saline (PBS) and filtered through a 70-μm filter. Cell suspensions were stained with phycoerythrin (PE/Cy7)-conjugated anti-CD31 (Ebioscience 25-0311), Biotin-conjugated anti-CD144 (Biolegend; 328120), anti-CD45 microbeads (Milltenyi), with simultaneous detection of GFP, CFP, YFP, or PE-Texas Red. Flow cytometry analysis and cell sorting was performed on a BD FACSAria (Becton Dickinson) cell sorting system under 20 psi with a 100-μm nozzle. In analyses, dead cells and cell debris were excluded by gating the population according to LIVE/DEAD Aqua Fixable Dead Cell Stain (Invitrogen) and using forward and side light scatters. The number of positive cells were compared with the number of cells positive in the staining with the IgG isotype controls (BD PharMingen) and determined with FACSAria flow cytometer (Becton Dickinson).

### Immunofluorescence Staining

Tissues were fixed in 4% paraformaldehyde at 4°C. Samples were prepared for embedding by soaking in 30% sucrose in PBS, and then quick-frozen in optimum cutting temperature (OCT) compound. Frozen sections (5–8 μm) were then blocked for 30 mins with 10% bovine serum albumin (BSA) and 2% goat serum followed by incubation with primary antibody for 12–16 hours. For immunostaining on sections from multi-colored mice, Alexa 647 or 750 conjugated antibody (1:1000) was used as a secondary stain for 1 hour (Invitrogen), and was visualized in the far-red channel (Cy5 or Cy7). Fluorescent images were taken with a Leica DM400B microscope (Leica Microsystems).

### Cell counting

To quantitatively assess clone size, defined by single color segments of blood vessels uninterrupted by any single cell of another color, we counted the number of contiguous colored cells with nuclei in each clone per section. The peak and mean clone sizes from serial sections were quantified.

### RNA Extraction and Gene Set Enrichment Analysis

Endothelial cells were FACS-sorted and total RNA was isolated by TRIzol extraction, labeled, and hybridized to Affymetrix microarrays (Mu430v2) as previously described. Each common reference sample was normalized to publically available Affymetrix mouse arrays (~ 20,000), and for each probeset, the dynamic range was calculated as the difference between the lowest and the highest expression values and normalized as described in (26). Microarray data may viewed under the Gene Expression Omnibus accession number GSE38461.

### Statistics

All data are presented as mean +− standard error (SE). For two group comparisons, two-tailed Student's t test was used. Chi-square tests were employed to examine the

compositional bias of countable clones in independent samples, and a p-value less than 0.05 was considered significant.

## Results

### Multicolor Lineage Tracing Analysis of Tumor Vascularization

To investigate the clonal origin and growth patterns of tumor blood vessels we utilized a multicolor Cre-dependent marker system (red, yellow, blue, and green) similar to Brainbow [9, 10]. In this model, Cre-mediated recombination, induced by tamoxifen, causes cells (and all of their progeny) to express one of four randomly assigned fluorescent proteins. We first analyzed clonal patterns under steady state conditions. Quantitative lineage tracing analysis 180 and 270 days after tamoxifen administration revealed minimal cellular proliferation in the steady state throughout small and medium arterial conduits, with median endothelial clone sizes of 1.2 and 1.4 (Figure S1), respectively. These findings are consistent with previous clonal tracing studies demonstrating mature vasculature to be relatively quiescent [11–14]. Areas of clonal proliferations were observed mostly at sites of vascular bifurcations in medium sized arteries, with clone sizes ranging from 8 – 15 endothelial cell divisions (Figure S1). These sites were characterized by single color segments uninterrupted by any single cell of another color, ruling out migration of other cells into the clonal region. The anatomic distribution of these sites suggest these expansions likely represent vascular remodeling induced by local hemodynamic changes.

We next used a lineage tracing strategy to investigate the spectrum of blood vessel clonality in response to pathologic stimuli. The tumor microenvironment is composed of numerous signaling molecules that induce changes in endothelial behavior to promote tumor growth and metastasis. To more completely understand the consequences of these angiogenic programs on the formation and maintenance of tumor vasculature *in vivo*, we engrafted Tamoxifen-pulsed VE-cadherin-CreERT2 Rainbow mice with syngeneic B16 melanoma. Melanomas are known to acquire a rich vascular network through the release of diffusible activators of angiogenesis [15]. Four weeks following engraftment of tumor, blood vessels were abundant within the tumor microenvironment. Clonal analysis of infiltrating tumor stromal elements (hematopoietic, fibroblast, and nerve) revealed a heterogeneous patterning with multiple colored clones equally represented (Figure 1a, 1d–e). In marked contrast, the clonal composition of infiltrating tumor vasculature was mono-to- oligoclonal, with large fields of single colored capillaries observed on cross sectional imaging (Figure 1b–c). Quantitative analysis demonstrated a mean clone size of 15.1 [3.6] compared to 1.2 [0.99] in adjacent structures (Table I).

To further characterize and quantify the contribution of individual clones, we next utilized a $Lin^-$, FSC intermediate, $CD144^+$ $CD31^+$ gating scheme on fluorescence activated cell sorting (FACS) to isolate single cells from suspensions of enzymatically digested tumor (Figure 2). Using this approach, we could detect and quantify Cre-induced fluorescent labeling specifically within the tumor vasculature across an entire engrafted tumor sample. Quantitative analysis by FACs demonstrated the distribution of clonality in the early period following engraftment was polyclonal, with relatively equal frequencies of fluorescent proteins (Figure 1d–e, Figure 2 a,d, Table I). Over extended periods, however, a subset of

endothelial cells increased in size over time, giving rise to large clones that contribute substantially to the overall tumor vasculature (Figure 2b, c). A 40 day chase revealed a mean clone size of 40.2 [53.9], with peak clone sizes varying widely up to 157.3, indicating large fields of single colored capillary networks (Table I). At these later time points, 79.7% (+/− 16) of all $CD45^{-}$ $CD31^{+}CD144^{+}$ endothelial cells were a single color, consistent with ever fewer but larger clones dominating the micro environmental landscape (Figure 2d).

## Stepwise progression of lineage restricted tissue resident progenitors

The above experiments suggested the clonal composition within evolving tumor microenvironments undergoes dynamic changes in response to angiogenic cues. These findings support a model where founder clones ($F_0$) diminish in frequency and are replaced by sub-clones ($F_1$) as tumors evolve. To explore this possibility, we isolated endothelial subsets, distinguished functionally by the magnitude of their contribution to the microenvironment, for gene expression profiling. Microarray analysis of FACS-isolated Lin-FSC low, $CD144^{+}$ $CD31^{+}$ founder ($F_0$) and sub-clone ($F_1$) endothelial cells from adult mice demonstrated that $F_0$ and $F_1$ endothelial cells shared a high degree of transcriptome-wide similarity ($R^2 = 0.92$) and similar expression of endothelial-related genes—such as CD144, Flt1, KDR, VWF, ITGB3, and the ETS transcription factor ETV6 (Figure 3 a–b). However, key differences in transcript expression were present, including differential expression of Met, Tie1, VCAM1, VEGFB, and SELE among many others (Figure 3c).

## Clonal evolution within the tumor microenvironment influences tumor immune function

One of the biological themes to emerge from this list is a loss in expression of functionally significant primary lymphocyte adhesion molecules. As tumor microenvironments mature, we find strong evidence for downregulation of SELE, MAdCAM-1, VCAM-1, ICAM-1, and ICAM-4—endothelial adhesion molecules that promote lymphocyte homing (Figure 3c). We note the interaction between endothelial cell adhesion molecules and lymphocyte homing receptors, is a key determinant in the infiltration of tumors by different subsets of lymphocytes and down regulation of these pathways has been associated with tumor outgrowth. Based on these findings, we hypothesized the consequences of clonal evolution within the tumor microenvironment in the expressed genetic program may well influence tumor immune function. In addition to the downregulation of key lymphocyte adhesion molecules, we also observe strong evidence for decreases in expression of lymphocyte chemokines CXCL16, CXCL13, CXCL12, CXCL9, CXCL10, CCL19 and inflammatory cytokines IL-15 (Natural Killer Cell and T cell), IL-11 (Monocyte/Macrophage), and G-CSF (Granulocyte/Dendritic Cell) (Figure 3C). The loss of pro-inflammatory cytokine and chemokine expression was associated with decreases in class I MHC expression and diminished expression of costimulatory molecules CD40 and ICOSL (Figure 3c).

## Enhanced autocrine signaling and the activation of alternative angiogenic programs

An additional biologic theme to emerge from our clonal analysis is a shift from paracrine to autocrine signaling as tissue microenvironments evolve. We see strong evidence for upregulation of self-sustaining growth signal networks; ($F_1$) sub-clone endothelial cells upregulate angiogenic ligands VEGF and VEGFB and their counter-receptor FLT1, as well as, the WNT receptor FZD7 and its ligand WNT5A (Table S1). These pathways have been

associated with tumor angiogenesis and reflect a shift from bidirectional supportive interactions between tumor and blood vessel to autonomous blood vessel growth. Furthermore, these changes are accompanied by activation of alternative angiogenic programs such as upregulation of the Hepatocyte Growth Factor receptor (HGF), c-Met, on ($F_1$) sub-clone endothelial cells (Table S1). We note HGF levels contribute to the angiogenesis associated with several human cancers.

### Negligible contribution from circulating cells to tumor vasculature maintenance

Lastly, at no time point did we find evidence for contributions for either a hematopoietically derived cell or a circulating cell of any type to formation or maintenance of tumor vasculature in B16 engrafted tumors. Wild-type mice were surgically conjoined to mice expressing GFP under a ubiquitous (chicken β-actin) promoter. These mice develop full hematopoietic chimerism within a month. B16 tumors were engrafted into non-GFP animals and removed after 1 month for analysis. GFP+ cells were observed throughout the tumor microenvironment (Figure S2) but did not incorporate into any vascular structures (Figure S2). All GFP+ cells expressed the pan hematopoietic marker CD45. We found no evidence of contributions from circulating cells, of any type, to cell turnover within tumor blood vessels.

## Discussion

The present study adapts a unique technology—a multicolor Cre-dependent “rainbow” reporter mouse—to show the formation and maintenance of vasculature in response to pathologic stimuli undergoes dynamic changes in clonal architecture. By using lineage tracing that allows for the visualization and categorization of all infiltrating cells, we offer a new approach to shed light on the cellular framework underlying formation of aberrant tumor niches. While it is generally accepted clonal progression occurs in cancer, with each heritable change increasing competitive competence of the cancer clone vs. normal cell—the clonal dynamics of the surrounding tumor microenvironment are unknown. We provide evidence for large clonal expansions within an advanced tumor microenvironment. These clonal patterns are similar in character to the diversification, expansion, and ultimate selection within competitive microenvironments described in cancer-clone evolution. Furthermore, these findings parallel a number of recent reports that show distinct clonal patterns during homeostatic compared to pathologic settings. Two distinct progenitor pools have recently been reported to contribute to Intestinal maintenance and repair. Following radiation injury, a normally quiescent population of Bmi-1 expressing Intestinal Stem Cells outcompetes $Lgr5^+$ expressing cells to clonally repopulate intestinal crypt [16,]. While previous clonal tracing of homeostatic endothelium using X chromosome inactivation analysis indicates subpopulations of endothelial cells undergoes clonal proliferation [17, 18], it is still not determined whether clonogenic `winners' are mature endothelial cells, or whether they are distinct stem or progenitor-less mature cells that can give rise to clonal colonies of endothelium.

Our experiments have several potential implications. First, the evolution of sub-clones within the microenvironment is one pathway to allow cancer cells to remodel tissue

microenvironments to their competitive advantages. In the case of tumor vasculature, alterations in lymphocyte-recognition tip the intra-tumor balance toward tumor immune escape and tolerance. Down regulation of endothelial adhesion molecules SELE, MAdCAM-1, VCAM-1, ICAM-1, and ICAM-4 may well influence tumor immune function. Moreover, this cellular framework may underlie a current barrier to immunotherapy. Adoptive transfer of engineered T cells for the treatment of solid cancer relies on the intra-tumoral accumulation of T cells. Licensing microenvironmental homing in favor of lymphocyte trafficking may be one approach to optimize these therapies. Lastly, the developmental shift in transcriptomes in evolved sub-clones to alternative angiogenic programs may underlie escape mechanisms from current anti-angiogenic pharmacotherapies and suggests the vascular tumor microenvironment is a moving therapeutic target.

## Supplementary Material

Refer to Web version on PubMed Central for supplementary material.

## Acknowledgments

This study was supported by in part by a NIH fellowship K12 HL087746 from the National Heart, Lung, and Blood Institute to DC, and by grant U01 HL099999, and from R01 CA86065 to ILW.

Funding Sources: This study was supported by in part by a NIH fellowship K12 HL087746 from the National Heart, Lung, and Blood Institute to D.M. Corey, 2T32AR050942-06A1 to D.M. Corey, and by grant U01 HL099999, and from R01 CA86065 to I.L.Weissman.

## References

1. Stoner DS, Rinkevich B, Weissman IL. Heritable germ and somatic cell lineage competitions in chimeric colonial protochordates. Proceedings of the National Academy of Sciences of the United States of America. 1999; 96(16):9148–53. [PubMed: 10430910]
2. Ueno H, Turnbull BB, Weissman IL. Two-step oligoclonal development of male germ cells. Proceedings of the National Academy of Sciences of the United States of America. 2009; 106(1): 175–80. [PubMed: 19098099]
3. Lambertsson A. The minute genes in Drosophila and their molecular functions. Advances in genetics. 1998; 38:69–134. [PubMed: 9677706]
4. Morata G, Ripoll P. Minutes: mutants of drosophila autonomously affecting cell division rate. Developmental biology. 1975; 42(2):211–21. [PubMed: 1116643]
5. Weissman IL. Stem cells: units of development, units of regeneration, and units in evolution. Cell. 2000; 100(1):157–68. [PubMed: 10647940]
6. Johnston LA. Competitive interactions between cells: death, growth, and geography. Science. 2009; 324(5935):1679–82. [PubMed: 19556501]
7. Calabrese C, Poppleton H, Kocak M, Hogg TL, Fuller C, Hamner B, et al. A perivascular niche for brain tumor stem cells. Cancer cell. 2007; 11(1):69–82. [PubMed: 17222791]
8. Beck B, Driessens G, Goossens S, Youssef KK, Kuchnio A, Caauwe A, et al. A vascular niche and a VEGF-Nrp1 loop regulate the initiation and stemness of skin tumours. Nature. 2011; 478(7369): 399–403. [PubMed: 22012397]
9. Rinkevich Y, Lindau P, Ueno H, Longaker MT, Weissman IL. Germ-layer and lineage-restricted stem/progenitors regenerate the mouse digit tip. Nature. 2011; 476(7361):409–13. [PubMed: 21866153]
10. Livet J, Weissman TA, Kang H, Draft RW, Lu J, Bennis RA, et al. Transgenic strategies for combinatorial expression of fluorescent proteins in the nervous system. Nature. 2007; 450(7166): 56–62. [PubMed: 17972876]

11. Schwartz SM, Benditt EP. Cell replication in the aortic endothelium: a new method for study of the problem. Laboratory investigation; a journal of technical methods and pathology. 1973; 28(6): 699–707.
12. Caplan BA, Schwartz CJ. Increased endothelial cell turnover in areas of in vivo Evans Blue uptake in the pig aorta. Atherosclerosis. 1973; 17(3):401–17. [PubMed: 4123526]
13. Schwartz SM, Benditt EP. Clustering of replicating cells in aortic endothelium. Proceedings of the National Academy of Sciences of the United States of America. 1976; 73(2):651–3. [PubMed: 1061164]
14. Engerman RL, Pfaffenbach D, Davis MD. Cell turnover of capillaries. Laboratory investigation; a journal of technical methods and pathology. 1967; 17(6):738–43.
15. Ria R, Reale A, Castrovilli A, Mangialardi G, Dammacco F, Ribatti D, Vacca A. Angiogenesis and progression in human melanoma. Dermatology research and practice. 2010; 2010:185687. [PubMed: 20631829]
16. Yan KS, Chia LA, Li X, Ootani A, Su J, Lee JY, et al. The intestinal stem cell markers Bmi1 and Lgr5 identify two functionally distinct populations. Proc Natl Acad Sci U S A. 2012; 109(2):466–71. [PubMed: 22190486]
17. Pearson TA, Dillman JM, Heptinstall RH. The clonal characteristics of human aortic intima. Comparison with fatty streaks and normal media. Am J Pathol. 1983; 113(1):33–40. [PubMed: 6624876]
18. Chung IM, Schwartz SM, Murry CE. Clonal architecture of normal and atherosclerotic aorta: implications for atherogenesis and vascular development. Am J Pathol. 1998; 152(4):913–23. [PubMed: 9546352]

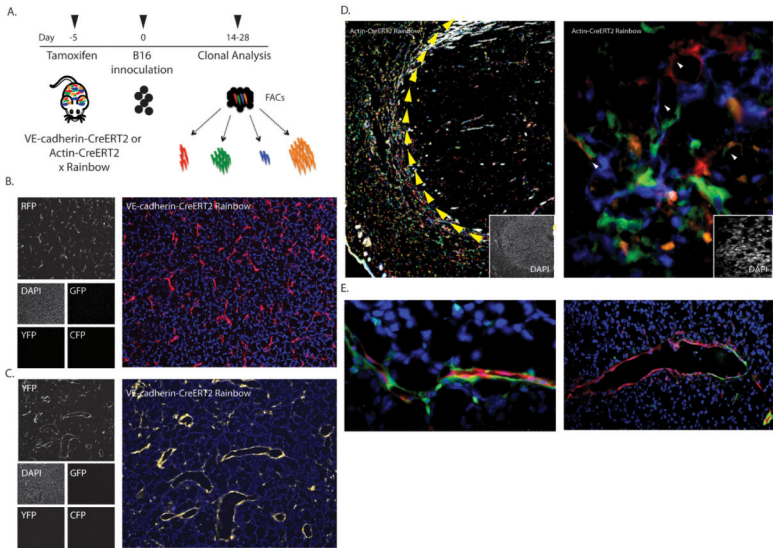


**Figure 1. Tumor Vascularization Follows a Pattern of Mono- to OligoClonal Expansion**

**(a)** Schematic of clonal analysis experiments. Syngeneic melanomas were injected subcutaneously into a multi-color reporter mouse (VE-cadherin-CreERT2 or Actin-Cre-ERT2 x Rainbow) to induce tumor vascularization. Tumors were analyzed for clonality by tissue section or enzymatically dissociated into single cell suspensions for FACs analysis on days 14–40. (**b–c**) Representative tissue sections from VE-cadherin-CreERT2 Rainbow tumors demonstrate large expansions of single colored fields of tumor vasculature dominating the microenvironmental landscape at day 28 (RFP top and YFP bottom). **(d)** Histologic section through Actin-CreERT2 Rainbow reporter mouse engrafted with B16 melanoma showing a heterogeneous clonal pattern of infiltrating stromal elements (colored) within a dense uncolored tumor mass (tumor border outlined with yellow arrows) 14 days after inoculation (DAPI stain lower corner). **(e)** Composite images from VE-cadherin-CreERT2 Rainbow mice 14 days after inoculation showing multiple clones contributing to tumor vasculature.

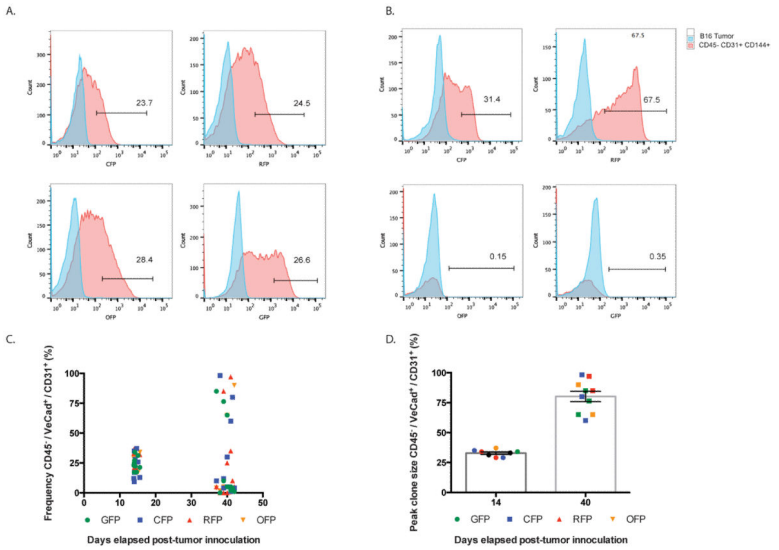


**Figure 2. Fluorescence-Activated Cell Sorting (FACS) Analysis of B16 Melanoma VE-cadherin-CreERT2 Rainbow Blood Vessels**

**(a)** FACs plots from $CD45^{-}CD31^{+}CD144^{+}$ tumor derived endothelial cells from a B16 tumor sample inoculated 14 days prior demonstrate relatively equal frequencies of fluorescent proteins. **(b)** FACs plots from $CD45^{-}CD31^{+}CD144^{+}$ tumor derived endothelial cells inoculated 40 days prior. At later time points, a subset of endothelial cells contribute substantially to the overall tumor vasculature. **(c)** Summary of FACs analyses showing frequency of $RFP^{+}$, $CFP^{+}$, $YFP^{+}$, or $GFP^{+}$ $CD45^{-}CD31^{+}CD144^{+}$ tumor derived endothelial cells (n= 10 tumor samples) at two time-points following inoculation. **(d)** Summary of FACs analyses of peak clone size from (n = 10) B16 tumor samples at two time points following inoculation. 79.7% (+/− 16) of all $CD45^{-}CD31^{+}CD144^{+}$ tumor derived endothelial cells are a single color.

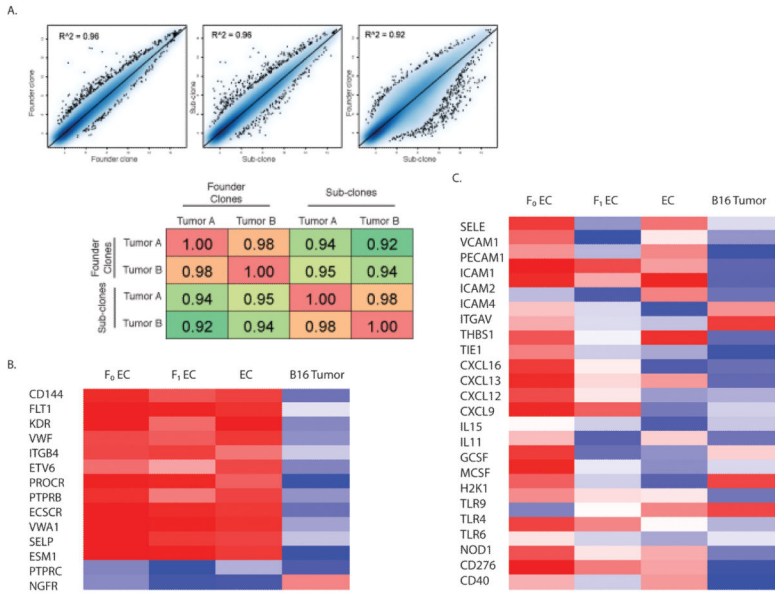


**Figure 3. Transcriptional profiling within the vascular tumor microenvironment**

Examination of gene expression from FACS-isolated Lin-FSC low, $CD45^{-}CD31^{+}CD144^{+}$ founder ($F_0$) and sub-clone ($F_1$) endothelial cells isolated from b16 mouse Melanoma tumors. **(a)** Microarray analysis of ($F_0$) and ($F_1$) endothelial cells across tumors demonstrate a high degree of transcriptome-wide similarity ($R^2 = 0.99$). (**b**) Correlation matrix demonstrate divergence in transcriptomes ($R^2 = 0.92$) between ($F_0$) and ($F_1$) clones. **(c)** Heat map from microarray analysis of endothelial (left) and lymphocyte adhesion and chemokine gene sets (right).

## Table I

### Clonal analysis of tumor vasculature

The peak clone size, defined by single color segments of blood vessels uninterrupted by any single cell of another color, were quantified at early and late time points following b16 mouse Melanoma engraftment. A 40 day chase revealed a mean clone size of 40.2 [53.9], with peak clone sizes varying widely up to 157.3, indicating large fields of single colored capillary networks.

| | 14 day pulse | | 40 day pulse | |
|---|---|---|---|---|
| | **Tumor vasculature** | **Non-tumor vasculature** | **Tumor vasculature** | **Non-tumor vasculature** |
| Mean clone size | 15.1 [3.6] | 1.2 [0.99] | 40.2 [53.9] | 1.3 [1.4] |
| Peak clone size | 20 | 8 | 157.3 | 12 |